ORIGINAL PAPER



Aqueous Synthesis of Pd–M (M = Pd, Pt, and Au) Decahedra with Concave Facets for Catalytic Applications

Hongwen Huang^{1,2,3} · Ruhui Chen⁴ · Maochang Liu¹ · Jinguo Wang⁵ · Moon J. Kim⁵ · Zhizhen Ye² · Younan Xia^{1,4,6}

Published online: 6 February 2020 © Springer Science+Business Media, LLC, part of Springer Nature 2020

Abstract

Noble-metal nanocrystals with structural features such as high-index facets and twin defects on the surface are desirable for various catalytic applications. Here we report an aqueous route to the facile synthesis of Pd–M (M=Pd, Pt, and Au) decahedra covered with concave facets by controlling the deposition and diffusion of M atoms on Pd decahedral seeds. Our mechanistic studies indicate that the preferential deposition of M atoms on the twin boundaries of Pd decahedral seeds under limited surface diffusion is instrumental to their evolution into decahedra enclosed by concave facets. Due to the presence of high-index facets and twin boundaries on the surface, the Pd concave decahedra show enhanced catalytic activity towards formic acid oxidation. The present work not only offers a general route to the facile synthesis of decahedral nanocrystals with concave facets but also provides an additional knob for enhancing the catalytic performance of noble-metal nanocrystals.

Keywords Palladium · Concave surface · High-index facet · Seed-mediated growth · Formic acid oxidation

1 Introduction

Noble-metal nanocrystals play an indispensable role as catalysts in a myriad of industrially important reactions or processes, including hydrogenation [1, 2], dehydrogenation

Electronic supplementary material The online version of this article (https://doi.org/10.1007/s11244-020-01235-w) contains supplementary material, which is available to authorized users.

- Younan Xia younan.xia@bme.gatech.edu
- The Wallace H. Coulter Department of Biomedical Engineering, Georgia Institute of Technology and Emory University, Atlanta, Georgia 30332, USA
- State Key Laboratory of Silicon Materials, Department of Materials Science and Engineering, Zhejiang University, Hangzhou 310027, Zhejiang, People's Republic of China
- Ollege of Materials Science and Engineering, Hunan University, Changsha 410082, Hunan, People's Republic of China
- School of Chemistry and Biochemistry, Georgia Institute of Technology, Atlanta, Georgia 30332, USA
- Department of Materials Science and Engineering, University of Texas at Dallas, Richardson, Texas 75080, USA
- School of Chemical and Biomolecular Engineering, Georgia Institute of Technology, Atlanta, Georgia 30332, USA

[3, 4], C–C coupling [5], and electrochemical oxidation of fuels based on small molecules such as hydrogen gas, formic acid, ethanol, and methanol [6–8]. Previous studies have established that the catalytic activity and/or selectivity of such nanocrystals are highly dependent on their composition, size, and shape or crystallographic facets exposed on the surface [9, 10]. Accordingly, engineering these parameters has become a central theme of research in the design and rational production of noble-metal nanocrystals with substantially enhanced catalytic performance.

Recently, nanocrystals with a concave surface have attracted increasing interest owing to their enhanced catalytic performance associated with the high-index facets that typically contain high densities of active sites in the form of atomic steps, kinks, and edges [11–13]. For example, Pd concave nanocubes enclosed by high-index facets have been reported with improved specific activity towards the electro-oxidation of formic acid, which was almost twice that of the conventional nanocubes [5]. To date, great success has been achieved in preparing a variety of noble-metal nanocrystals characterized by a concave surface, with notable examples including concave nanocubes [14-16], tetrahedra [17, 18], and octahedra [19-21]. All of these nanocrystals, however, have a single-crystal structure. If one could synthesize multiplytwinned nanocrystals encased by a concave surface, they



are expected to exhibit more marvelous catalytic performance owing to the presence of both high-index facets and twin boundaries. So far, there are only a few reports on the synthesis of this unique class of nanocrystals [22–24]. Specifically, Xu and co-workers demonstrated the synthesis of Au/Pd bimetallic concave, branched nanostructures via seed-mediated growth method using the rod-shaped Au/Pd nanoparticles as seeds in an aqueous solution [22]. Through careful manipulation of the reduction kinetics and thus the site of preferential overgrowth, Wang and coworkers reported an aqueous-solution synthesis of a mix of Pd concave nanorods (24%), concave right bipyramids (42%), and concave nanocubes (34%) [23]. With Pd decahedral nanocrystals serving as seeds, our group demonstrated a polyol route to the synthesis of Pd–Pt core-shell concave decahedra with substantially enhanced activity towards the oxygen reduction reaction [24]. Despite the progress, these approaches tend to suffer from problems such as low purity and/or relatively high reaction temperatures (above 200 °C). We still lack a facile and general method for the synthesis of nanocrystals featuring a multiply-twinned structure and a concave surface in an aqueous system and at a relatively low temperature. In this work, we report a general protocol for the facile synthesis of Pd-M (M = Pd, Pt, and Au) concave decahedra by controlling the overgrowth of Pd decahedral seeds. By deliberately manipulating the reduction kinetics relative to surface diffusion, the deposition of M atoms could be largely confined to the twin boundaries on the surface of a seed for the generation of concave facets. We also evaluated the catalytic activity of the as-obtained Pd concave decahedra by employing the electro-oxidation of formic acid (FAO) as a model reaction. Owing to the presence of both high-index facets and twin boundaries on the surface, the Pd concave decahedra exhibited an enhanced specific activity relative to those of Pd decahedra and octahedra.

2 Experimental Section

2.1 Chemicals and Materials

Diethylene glycol (DEG, \geq 99.0%), sodium tetrachloropalladate(II) (Na₂PdCl₄, 99.998%), potassium tetrachloroplatinate(II) (K₂PtCl₄, 98.0%), chloroauric acid trihydrate (HAuCl₄·3H₂O, \geq 99.9%), sodium sulfate (Na₂SO₄, \geq 99.0%), citric acid (CA, \geq 99.5%), poly(vinyl pyrrolidone) (PVP, MW \approx 55,000), and L-ascorbic acid (AA, \geq 99.0%) were all obtained from Sigma-Aldrich. All the chemicals were used as received. Deionized (DI) water with a resistivity of 18.2 M Ω cm was used throughout the experiments.

2.2 Synthesis of Pd Decahedral Seeds

The Pd decahedra seeds were prepared using the method we previously developed [25]. Briefly, 2.0 mL of DEG containing 80 mg of PVP and 40 mg of Na_2SO_4 was heated at 105 °C under magnetic stirring for 20 min. Meanwhile, 15.5 mg of Na_2PdCl_4 was dissolved in 1.0 mL of DEG and added into the above solution with a pipette. The reaction was allowed to proceed for 2 h to obtain Pd decahedra with an average size of 9.5 nm. After collection by centrifugation, the decahedral seeds were washed once with acetone and then twice with water before re-dispersion in water for further use.

2.3 Synthesis of Pd Concave Decahedra

In a standard synthesis, 8.0 mL of an aqueous mixture containing Pd decahedral seeds (0.02 mg/mL), 105 mg of PVP, and 60 mg of AA was heated at 95 °C for 15 min in a 25 mL three-neck flask under magnetic stirring. Subsequently, 3.0 mL of aqueous Na₂PdCl₄ (1.2 mg/mL) was titrated into the above solution at a rate of 0.3 mL/h using a syringe pump. The product was collected by centrifugation at 13,200 rpm for 10 min and washed twice with water prior to further characterization.

2.4 Synthesis of Pd-Pt Concave Decahedra

Similar to the synthesis of Pd concave decahedra, 3.0 mL of an aqueous mixture containing Pd decahedral seeds (0.15 mg/mL), 35 mg of PVP, and 60 mg of CA was heated at 95 °C for 15 min. Then, 1.0 mL of aqueous K₂PtCl₄ solution (3 mg/mL) was quickly injected into the solution with a pipette. After the reaction had proceeded for 3 h, the solid product was collected by centrifugation.

2.5 Synthesis of Pd-Au Concave Decahedra

The experimental protocol was the same as what was used in the synthesis of Pd concave decahedra except that $6.0 \, \text{mL}$ of aqueous HAuCl_4 (0.4 mM) was titrated into the reaction system with a syringe pump at a rate of $3.0 \, \text{mL/h}$ while the synthesis was kept in an ice-water bath (0 °C) to limit the surface diffusion of Au atoms.

2.6 Characterization

The transmission electron microscopy (TEM) images were obtained using a Hitachi HT7700 microscope operated at 120 kV. The high-resolution TEM (HRTEM) and high-angle annular dark-field scanning TEM (HAADF-STEM) images were acquired using a JEOL JEM 2200FS STEM/TEM



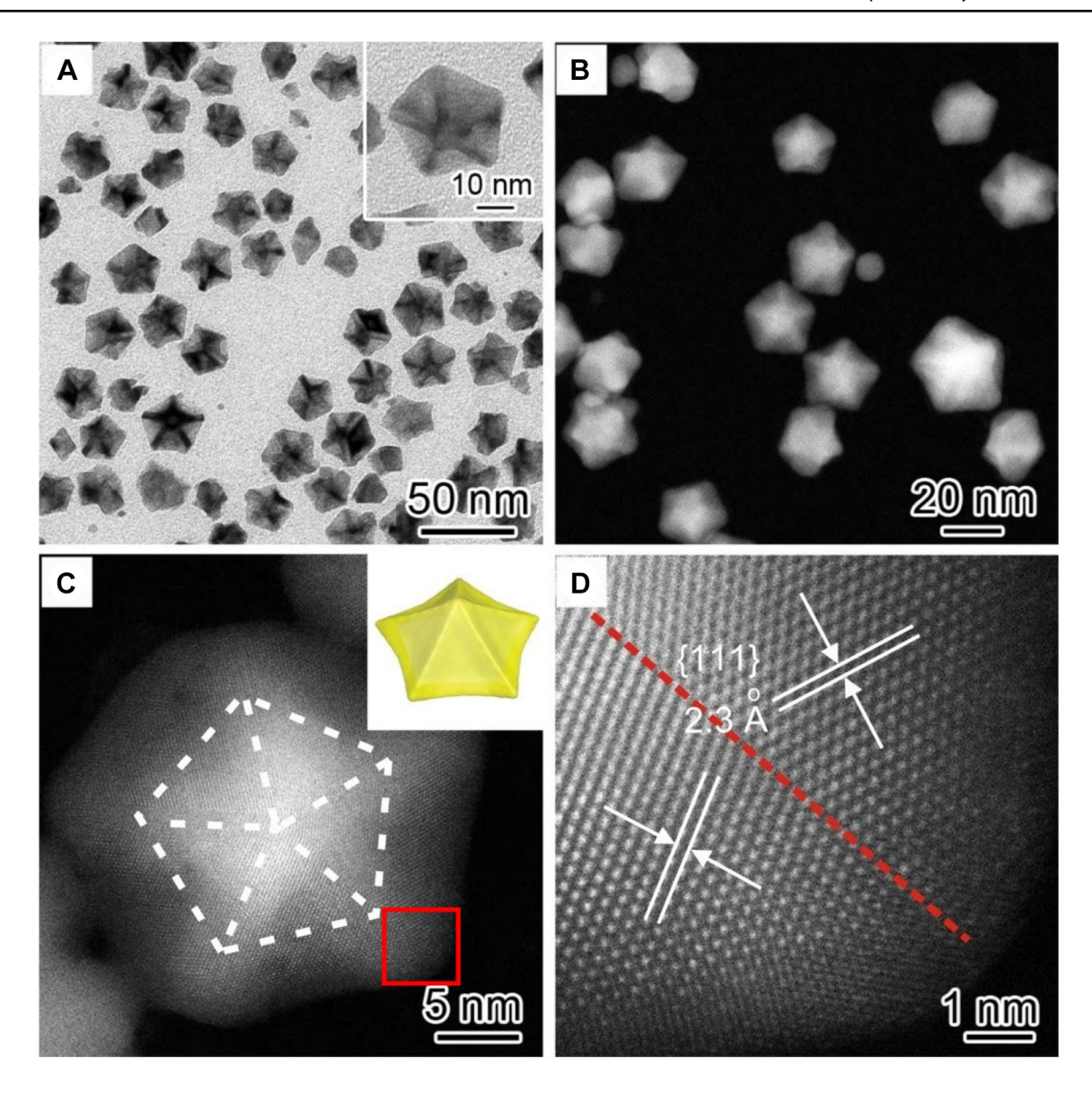


Fig. 1 Electron microscopy characterizations of the Pd concave decahedra prepared using the standard protocol. **a** TEM and **b** HAADF-STEM images of the Pd concave decahedra. **c** HAADF-STEM image of an individual Pd concave decahedron. The dashed lines indicate the dimensions of the Pd decahedral seed used for the synthesis of

the Pd concave decahedra. The inset shows a model of the concave decahedron. \mathbf{d} Atomic-resolution HAADF-STEM image of the area marked by the red box in \mathbf{c} , showing two sets of {111} planes separated by a twin plane as indicated by the red dashed line

microscope. The concentrations of metal ions were determined using inductively-coupled plasma mass spectrometry (ICP-MS, Perkin Elmer, NexION 300Q).

2.7 Electrochemical Measurements

Pd decahedra and octahedra were synthesized by following the protocols we previously reported and used as references for benchmarking the catalytic activity of the Pd concave decahedra [7, 25]. All electrochemical characterizations were carried out in a three-compartment cell connected to an electrochemical workstation (CHI 600E, CH Instruments).

An Ag/AgCl electrode and a Pt mesh served as the reference and counter electrodes, respectively. The applied potentials in the measurements were presented with reference to the reversible hydrogen electrode (RHE). Prior to the measurements, the catalyst ink was prepared by dispersing the asprepared Pd concave decahedra, decahedra, or octahedra in 1.0 mL of water at a concentration of 0.2 mg/mL. 10 μ L of the suspension was then drop-cast on a pre-cleaned, glassy carbon electrode (Bioanalytical Systems) and dried in an oven at 50 °C for 10 min. Afterwards, 5 μ L of Nafion aqueous solution (0.05%) was deposited onto the electrode and allowed to dry in the same oven for another 10 min. Plasma



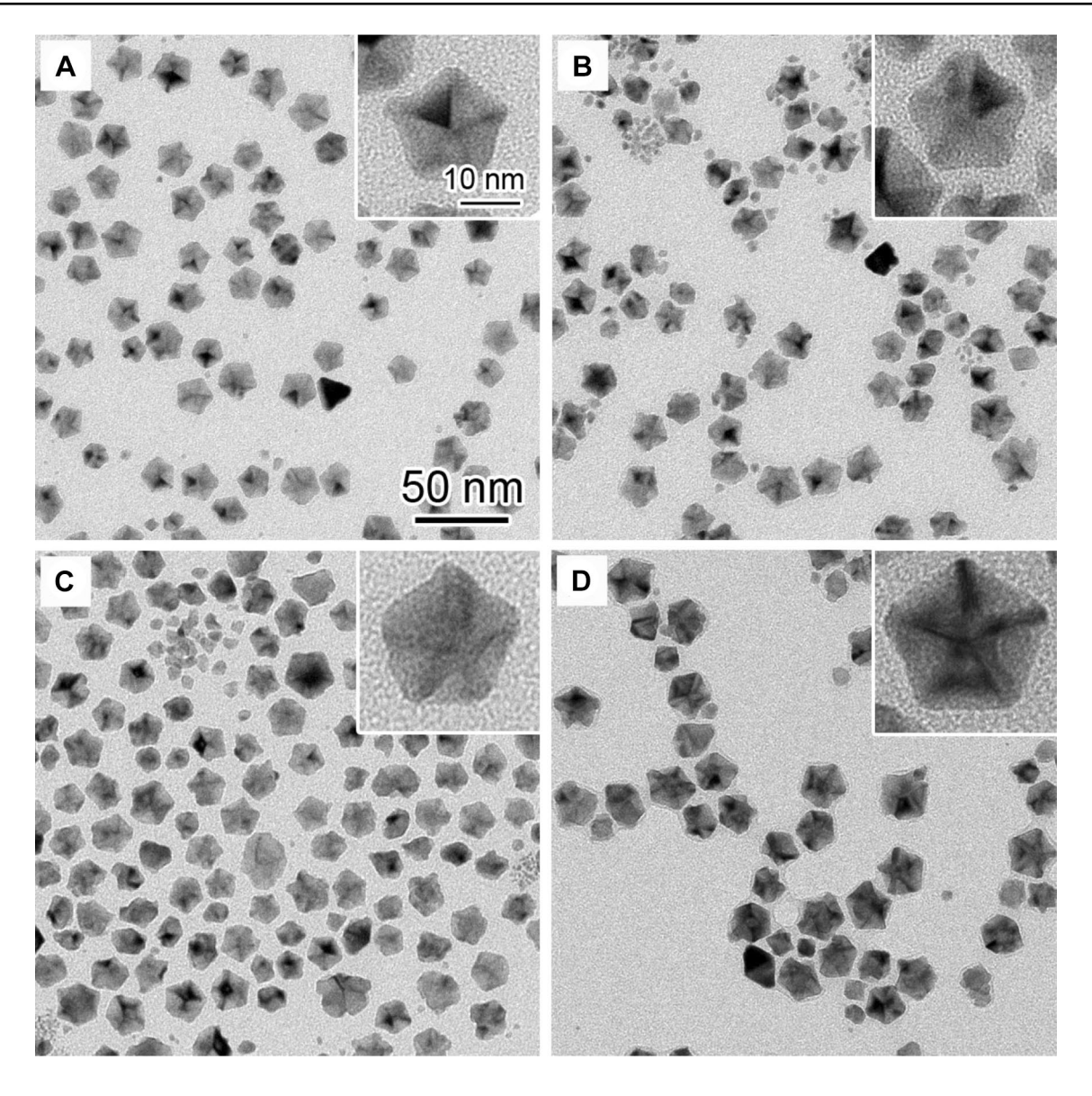


Fig. 2 TEM images of Pd concave decahedra obtained by adding different volumes of aqueous Na_2PdCl_4 into the synthesis: **a** 0.5, **b** 1.0, **c** 1.5, and **d** 2.0 mL. The insets show TEM images of individual nanocrystals at a higher magnification. The scale bars in **a** apply to all other panels

etching (PE-50, Plasma Etch) was then applied for 30 min to clean the surface of the catalyst. The FAO measurement was conducted by cycling the potential between 0.08 and 1.1 V for three cycles in a $\rm N_2$ -saturated aqueous solution containing 0.5 M HClO $_4$ and 0.5 M HCOOH at a scan rate of 50 mV/s. The electrochemically active surface area (ECSA) of the catalyst was derived by recording the cyclic voltammogram (CV) of Cu underpotential deposition (Cu_{UPD}) in an aqueous solution of 0.05 M $\rm H_2SO_4$ and 0.05 M CuSO $_4$ in the potential range of 0.4 to 0.7 V at a scan rate of 5 mV/s.

3 Results and Discussion

The Pd decahedral seeds with an average edge length of 9.5 nm (Fig. S1) were prepared by following a previously reported protocol [25]. In a typical synthesis of Pd concave decahedra, aqueous Na₂PdCl₄ (a precursor) was slowly titrated into a mixture containing PVP, AA, and the decahedral seeds. Since this Pd(II) precursor can be quickly reduced by AA at 95 °C, it is critical to have it slowly introduced into the reaction system dropwise in order to avoid homogeneous nucleation. The structural details of the as-obtained Pd nanocrystals were characterized by both TEM and HRTEM. As shown in Fig. 1a, Pd concave decahedra with an average edge length of about 16.3 nm could be produced with purity



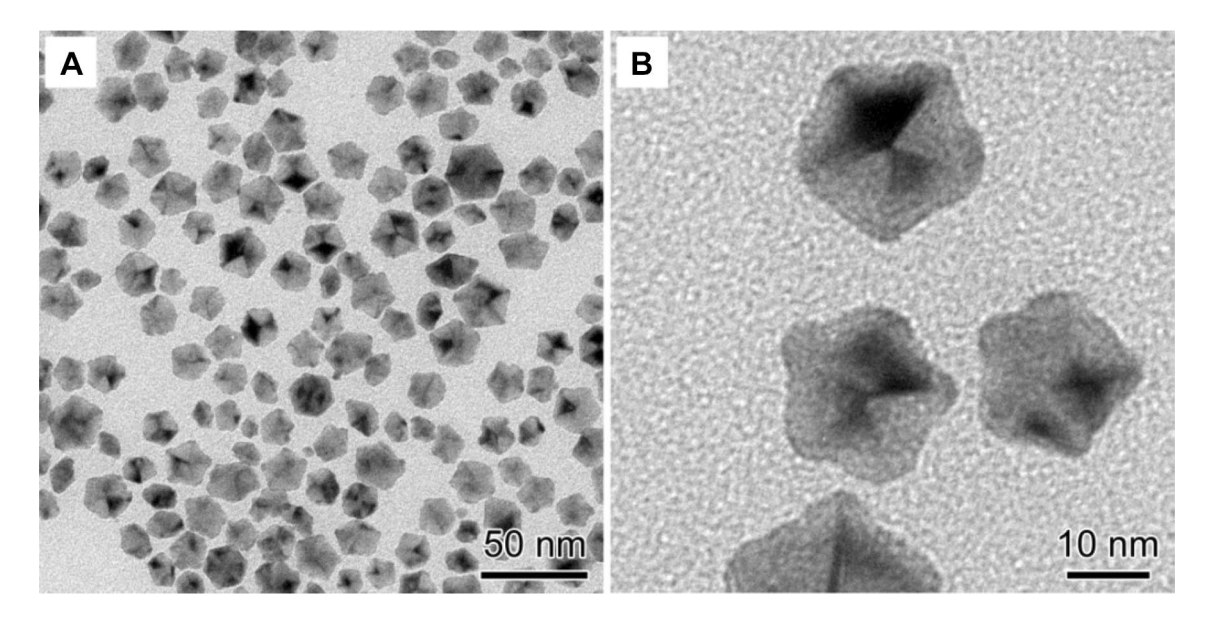


Fig. 3 a Low-magnification, and b high-magnification TEM images of the Pd-Pt concave decahedra

greater than 90%. The concave surface of the nanocrystals could be identified by the obvious contrast in thickness under TEM imaging as dark strips were clearly observed along the twin boundaries of each nanocrystal. Such a feature could be ascribed to the increase in thicknesses at the twin boundaries due to the preferential deposition of atoms at these sites. The inset of Fig. 1a shows a nanocrystal at a higher magnification, further confirming the concave, decahedral structure with protuberant twin boundaries. As shown by the HAADF-STEM image in Fig. 1b, five twin boundaries could be easily resolved on the particles because of their increased thickness and thus enhanced contrast, further attesting the concave surface. Figure 1c shows a HAADF-STEM image of a Pd concave decahedron and its corresponding 3D model in the inset. The pentagon marked by dashed lines indicates the dimension of the decahedral seed used for the synthesis. Based on the atomic-resolution HAADF-STEM image in Fig. 1d, it can be concluded that the twin defect of the decahedral seed, as marked by the red dashed line, was well preserved despite the overgrowth on the twin boundaries. The lattice fringes with a d spacing of 0.23 nm could be indexed to the {111} planes of Pd. These observations explicitly validated that penta-twinned Pd concave decahedra were successfully synthesized by controlling the overgrowth of Pd decahedral seeds.

To gain insight into the formation mechanism of the multiply-twinned concave structure, we monitored the morphological evolution of the Pd decahedral seeds by characterizing the samples obtained with the addition of different amounts of Na₂PdCl₄ into the same reaction mixture. As shown in Fig. 2a, when a small volume of Na₂PdCl₄ solution (0.5 mL, 1.2 mg/mL) was introduced into the reaction

mixture, the shape and size of the resultant Pd nanocrystals seemed to be almost identical to the initial decahedral seeds. However, a closer examination by TEM at a higher magnification (shown in the inset) clearly reveals the slightly protuberant corners and twin boundaries of the nanocrystal. These images also confirmed that the deposition of the newly formed Pd atoms onto the decahedral seed preferentially started from the corners and twin boundaries on the seed due to their greater surface free energy compared with the side faces. When 1.0 mL of the Na₂PdCl₄ solution was added, more obviously protuberant twin boundaries were observed for the Pd decahedral seeds (Fig. 2b). With the addition of more Na₂PdCl₄ (Fig. 2c, d), the Pd decahedral seeds gradually grew into larger nanocrystals with thicker twin boundaries. These results clearly demonstrated the preferential deposition of Pd atoms onto twin boundaries of the decahedral seeds was responsible for the generation of a concave surface on the nanocrystals. As schematically shown in Fig. S2, owing to the greater surface free energy of the twin boundaries on a decahedral seed, the Pd atoms derived from the reduction of Na₂PdCl₄ would preferentially nucleate from these sites. Of course, the as-deposited Pd atoms could migrate to other sites, such as the twin-free edges and {111} facets through surface diffusion. In this case, the ratio of atom deposition rate to adatom diffusion rate would determine the shape evolution of the growing nanocrystals [26]. Specifically, when the deposition rate was fast while the diffusion of adatoms across the surface was hindered, concave decahedra with protuberant twin boundaries would be achieved, as observed in Fig. 1.

The synthetic approach could also be adapted for bimetallic systems. In general, bimetallic nanocrystals not only



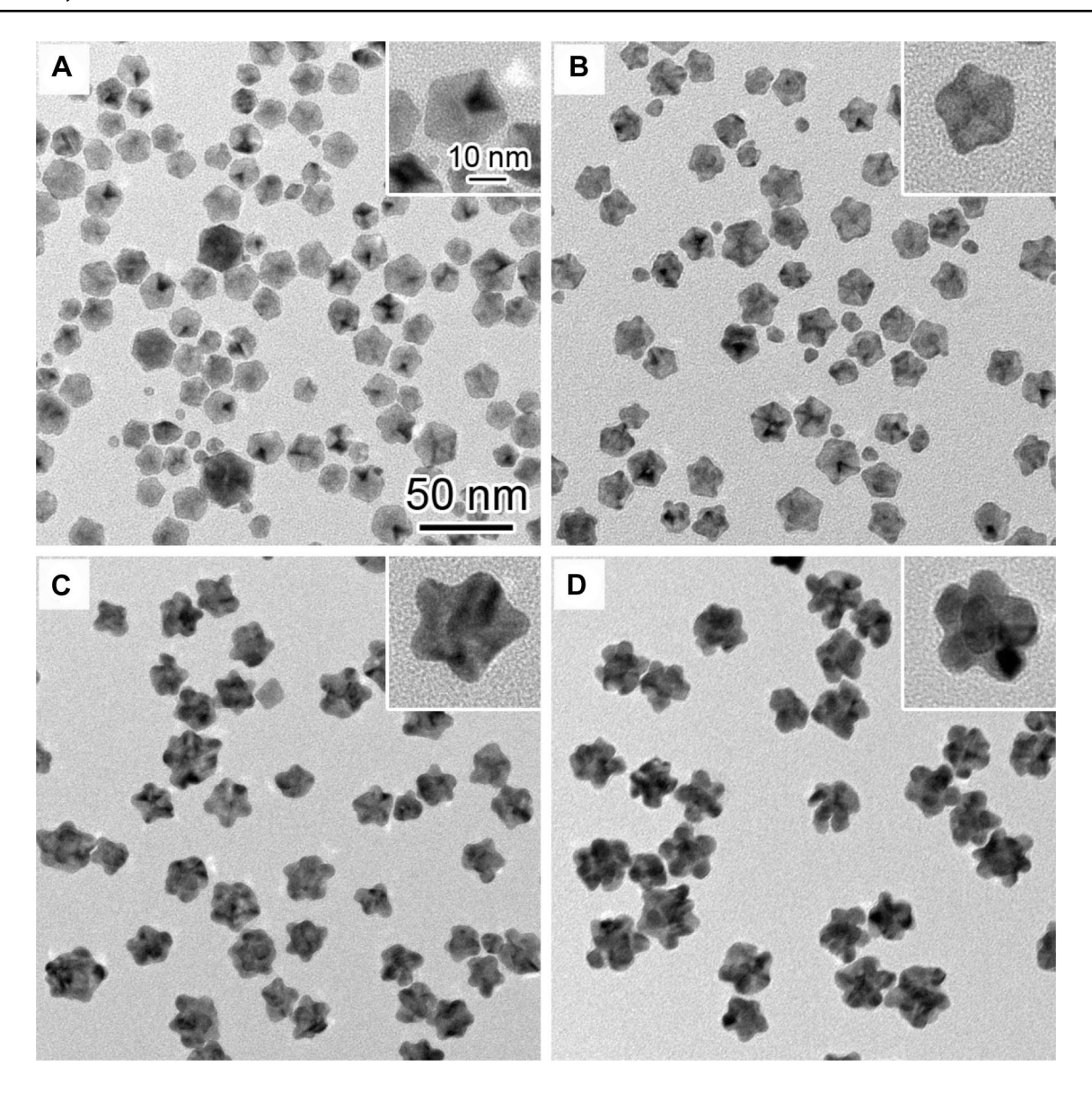


Fig. 4 TEM images of the Pd–Au concave decahedra obtained by adding $\bf a$ 0.2, $\bf b$ 1.0, $\bf c$ 3.0, and $\bf d$ 6.0 mL of aqueous HAuCl₄ into the reaction mixture. The insets show magnified images of individual nanocrystals. The scale bars in $\bf a$ apply to all other panels

exhibit a combination of the properties associated with the two metals but also can offer great enhancement due to electronic coupling between the different types of metal atoms [27]. In the first attempt, we extended the aqueous protocol to the synthesis of Pd–Pt bimetallic concave decahedra. Since the bonding energies increase in the order of $E_{\rm Pd-Pd}$ (136 kJ/mol) < $E_{\rm Pt-Pd}$ (191 kJ/mol) < $E_{\rm Pt-Pt}$ (307 kJ/mol), it is more difficult for Pt adatoms to diffuse across the surface of a preformed Pd decahedral seed. When a strong reducing agent such as AA is involved, the fast deposition of Pt atoms onto the seed would result in the formation of dendritic structures via the Volmer-Weber (or island) growth mode [28, 29]. Hence, to obtain Pd–Pt concave decahedra, we switched the reducing agent from AA to citric acid to

attain a weaker reducing power. As a result, the deposition rate of Pt atoms could be substantially slowed down to achieve the Frank-van der Merwe (or layer-by-layer) growth mode on the twin boundaries, preserving the twin defects on the seed while generating concave facets. In fact, the reducing power of citric acid was so low that the Pt(II) precursor could be added into the reaction system in one shot, rather than dropwise, without causing homogeneous nucleation. Figure 3 shows low- and high-magnification TEM images of the as-obtained Pd–Pt concave decahedra, where protuberant twin boundaries could be clearly observed. The ratio of Pt to Pd atoms was determined to be 0.13:1 by ICP-MS. As demonstrated in a related study [24], such a unique structure with Pt atoms situated on high-index facets and twin defects is



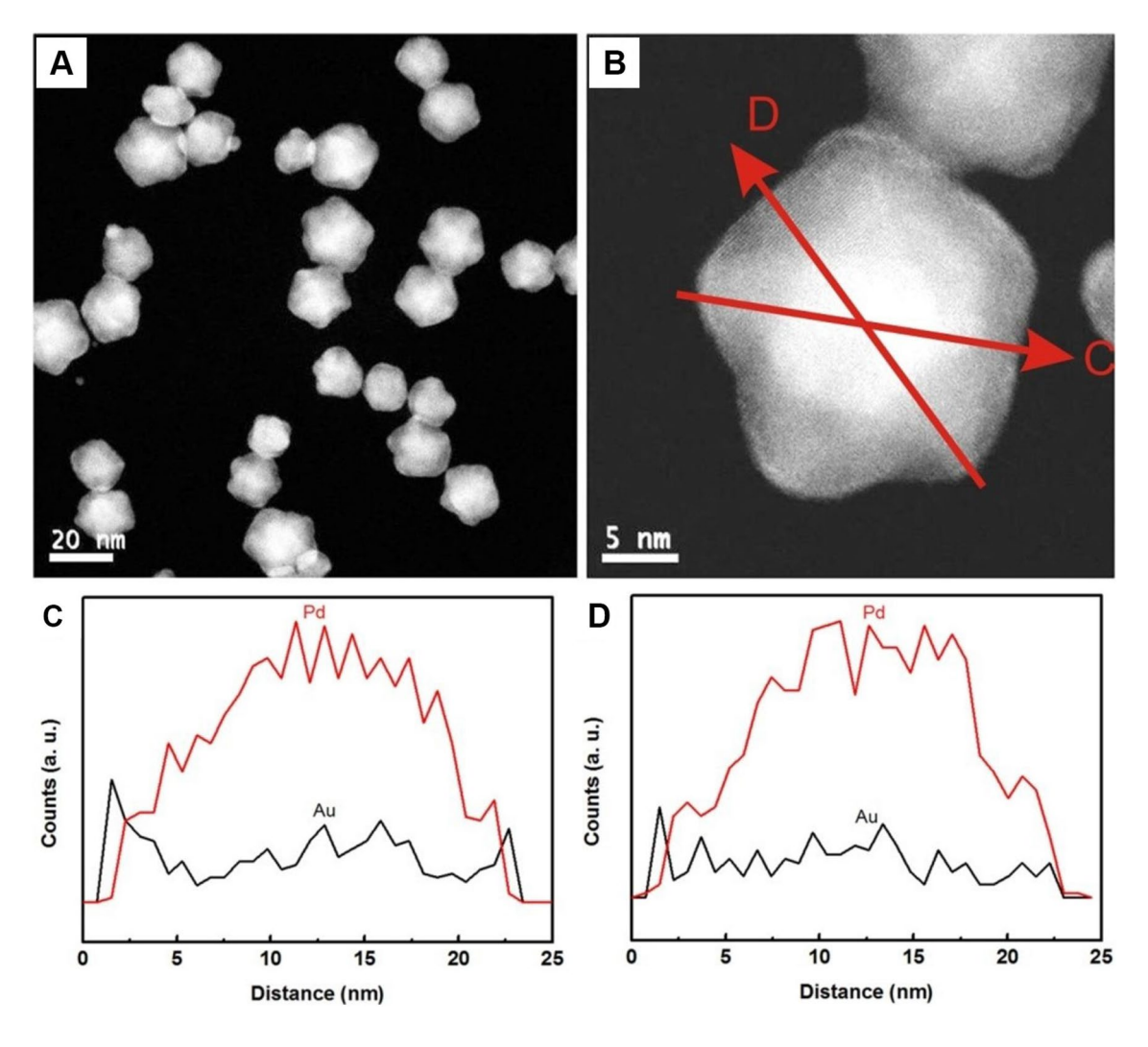


Fig. 5 Structural and composition characterizations of the Pd-Au nanocrystals obtained with the addition of 0.2 mL HAuCl₄ (0.4 mM). **a**, **b** HAADF-STEM images at different magnifications; **c**, **d** EDX line-scan spectrum recorded along the lines shown in **b**

well-suited for the development of low-Pt catalysts towards the oxygen reduction reaction [30].

The synthetic procedure for Pd-Au concave decahedra was similar to the synthesis of Pd concave decahedra, except that the synthesis had to be conducted at a low temperature of 0 °C to slow down the diffusion rate of Au adatoms on the Pd decahedral seeds. The shape evolution of the Pd-Au nanocrystals was investigated by imaging the nanocrystals obtained when different amounts of HAuCl₄ was introduced into the reaction mixture. As shown in Fig. 4a, when 0.2 mL of HAuCl₄ solution was added, some of the corners and twin boundaries on the decahedral seeds exhibited slight protuberance, which is consistent with what was observed during the synthesis of Pd concave decahedra. With more HAuCl₄ introduced into the reaction, the degree of protuberance on the twin boundaries of Pd-Au nanocrystals was intensified and the nanocrystals eventually evolved into a starfish shape when 6.0 mL of HAuCl₄ solution was injected (Fig. 4b-d). To further confirm the preferential deposition of Au atoms onto twin boundaries of the decahedral seeds, the sample shown in Fig. 4a was further characterized by HAADF-STEM combined with energy dispersive X-ray (EDX) spectrometry, as shown in Fig. 5. The EDX line-scan plots (Fig. 5c, d) acquired along the two arrows crossing the nanocrystal give a clear picture about the spatial distributions of Au atoms on the Pd decahedral seed. When moving from one of the corners of the decahedron along the twin boundary toward one of the twin-free edges, the line-scan plots confirm higher counts of Au at the sites close to the starting point. In other words, more Au atoms were deposited on the corners and twin boundaries of the concave decahedron than other regions close to the twinfree edges. The EDX analysis thus further supports the proposed mechanism, in which the preferential deposition of Au atoms on twin boundaries of Pd decahedral seeds contributed to the formation of the concave structure. It should be



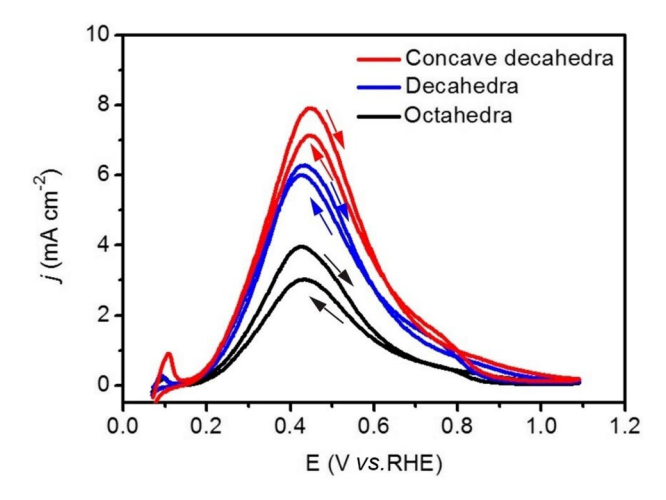


Fig. 6 Cyclic voltammetry curves of Pd concave decahedra (red), decahedra (blue), and octahedra (black) catalysts recorded at room temperature in a N_2 -saturated aqueous solution containing 0.5 M HClO $_4$ and 0.5 M HCOOH at a scan rate of 50 mV/s. The current densities were normalized to the corresponding ECSA of the catalysts

mentioned that the surface exposed at the protuberant twin boundaries is supposed to be covered by high-index facets because of the high densities of atom steps and kinks at these sites. However, the Miller indices of these high-index facets should differ from one to another because they arose from preferential deposition combined with limited diffusion instead of isotropic growth, no matter what composition the nanocrystal takes. Moreover, it is worth noting that the degree of concavity of the Pd-Au concave decahedra was much higher than that of Pd concave decahedra. The formation of starfish-like Pd-Au nanocrystals with five protuberant arms could be attributed to the fast reduction of HAuCl₄ precursor to Au atoms by AA, together with the slow diffusion rate of Au adatoms due to the low reaction temperature of 0 °C. Interestingly, different from the synthesis of Pd and Pd-Pt concave decahedra, it was found that the color of the reaction solution changed from pale yellow to purple during the formation of Pd–Au nanocrystals. As shown in Fig. S3, an absorption band located around 510–560 nm, originating from the localized surface plasmon resonance of Au [31], could be observed with increased intensity as more HAuCl₄ was added into the reaction mixture, suggesting the overgrowth of Au onto Pd decahedral seeds.

Owing to the presence of high-index facets and a multiply-twinned structure, the concave decahedra are expected to exhibit enhancement in catalytic activity. We evaluated the catalytic activity of the 16.3 nm-Pd concave decahedra by employing FAO as a model reaction. We benchmarked their activity against 9.5 nm-Pd decahedra (Fig. S1), and 20-nm Pd octahedra (Fig. S4) under the same experimental conditions. Since all of these nanocrystals were synthesized in the presence of PVP as a colloidal stabilizer, it is reasonable to

rule out the effect of surface capping on the catalytic activity for the establishment of an authentic correlation between the performance and surface atomic structure. Electrochemical CVs were used to measure the activities of these catalysts. Fig. S5 shows the CV curves for the Cu_{UPD} measured in a N₂-saturated aqueous solution containing 0.05 M H₂SO₄ and 0.05 M CuSO₄ at a scan rate of 5 mV/s. The characteristic Cu_{IIPD} current peaks for Pd decahedra and octahedra enclosed by the same {111} facets were observed at 0.52 and 0.53 V, respectively, with the peak of the octahedra being sharper than that of the decahedra. The difference could be ascribed to the presence of twin defects and slight truncation on the surface of Pd decahedra [32]. For the concave decahedra, an even broader peak was observed due to the presence of a number of unknown facets on the concave surfaces, in addition to the twin defects. Table S1 summarizes the ECSAs of these catalysts determined by integrating the stripping charges and assuming 460, 490, and 490 µC/cm² for a monolayer of Cu on the concave decahedra, decahedra, and octahedra, respectively [32]. Figure 6 shows the CVs normalized to the ECSAs of these catalysts. The Pd concave decahedra exhibited a specific catalytic activity with 26% and 100% enhancement relative to those of decahedra and octahedra, respectively (see Table S1 for detailed data). This data demonstrated that the high-index facets and multiply twinned structure could be combined to improve the catalytic activity of Pd nanocrystals towards FAO.

4 Conclusions

In summary, we have demonstrated an aqueous route to the facile synthesis of Pd concave decahedra using a kinetically controlled protocol in the presence of Pd decahedra as seeds. By investigating the shape evolution of the Pd decahedral seeds during a synthesis, it was proposed that the preferential deposition of Pd atoms onto the twin boundaries with a greater surface energy and the limited surface diffusion were responsible for the formation of Pd decahedra covered by concave facets. Based on the mechanistic understanding of Pd concave decahedra, we further extended this seeded growth strategy to the synthesis of Pd-Pt and Pd-Au concave decahedra, demonstrating the generality of this approach. Due to the presence of multiple twin defects and high-index facets, the as-obtained Pd concave decahedra showed enhanced catalytic performance towards FAO, with specific activity 1.3 and 2.0 times greater than those of Pd decahedra and octahedra, respectively. The present work not only provides a general approach to the facile synthesis of metal nanocrystals with a multiply-twinned structure and concave facets but also offers a new avenue for optimizing their catalytic performance.



Acknowledgements This work was supported in part by a research grant from the NSF (CHE1804970) and startup funds from Georgia Institute of Technology. As a visiting Ph.D. student from Zhejiang University, H. Huang was also partially supported by a Fellowship from the China Scholarship Council.

Compliance with Ethical Standards

Conflict of interest The authors declare no conflict of interest.

References

- Tsung CK, Kuhn JN, Huang W, Aliaga C, Hung LI, Somorjai GA, Yang P (2009) J Am Chem Soc 131:5816–5822
- Song S, Liu R, Zhang Y, Feng J, Liu D, Xing Y, Zhao F, Zhang H (2010) Chem Eur J 16:6251–6256
- 3. Ye H, Wang Q, Catalano M, Lu N, Vermeylen J, Kim MJ, Liu Y, Sun Y, Xia X (2016) Nano Lett 16:2812–2817
- 4. Chen Y, Yang X, Kitta M, Xu Q (2017) Nano Res 10:3811-3816
- Jin M, Zhang H, Xie Z, Xia Y (2011) Angew Chem Int Ed 50:7850–7854
- Chen X, Wu G, Chen J, Chen X, Xie Z, Wang X (2011) J Am Chem Soc 133:3693–3695
- Jin M, Zhang H, Xie Z, Xia Y (2012) Energy Environ Sci 5:6352–6357
- Hong JW, Kim Y, Kwon Y, Han SW (2016) Chem Asian J 11:2224–2239
- 9. Zhou K, Li Y (2012) Angew Chem Int Ed 51:602-613
- Xie S, Choi S, Xia X, Xia Y (2013) Curr Opin Chem Eng 2:142–150
- 11. Somoriai GA, Blakely DW (1975) Nature 258:580-583
- 12. Zhou ZY, Huang ZZ, Chen DJ, Wang Q, Tian N, Sun SG (2010) Angew Chem Int Ed 49:411–414
- 13. Chen A, Holt-Hindle P (2010) Chem Rev 110:3767-3804
- Zhang J, Langille MR, Personick ML, Zhang K, Li S, Mirkin CA (2010) J Am Chem Soc 132:14012–14014

- Yu T, Kim DY, Zhang H, Xia Y (2011) Angew Chem Int Ed 50:2773–2777
- Cheong S, Watt J, Ingham B, Toney MF, Tilley RD (2009) J Am Chem Soc 131:14590–14595
- Huang X, Tang S, Zhang H, Zhou Z, Zheng N (2009) J Am Chem Soc 131:13916–13917
- Xie S, Zhang H, Lu N, Jin M, Wang J, Kim MJ, Xie Z, Xia Y (2013) Nano Lett 13:6262–6268
- Xia X, Zeng J, McDearmon B, Zheng Y, Li Q, Xia Y (2011)
 Angew Chem Int Ed 50:12542–12546
- Zhu E, Li Y, Chiu CY, Huang X, Li M, Zhao Z, Liu Y, Duan X, Huang Y (2016) Nano Res 9:149–157
- Lu CL, Prasad KS, Wu HL, Ho JA, Huang MH (2010) J Am Chem Soc 132:14546–14553
- Zhang LF, Zhong SL, Xu AW (2013) Angew Chem Int Ed 52:645–649
- 23. Shao Z, Zhu W, Wang H, Yang Q, Yang S, Liu X, Wang G (2013) J Phys Chem C 117:14289–14294
- Wang X, Vara M, Luo M, Huang H, Ruditskiy A, Park J, Bao S, Liu J, Howe J, Chi M, Xie Z, Xia Y (2015) J Am Chem Soc 137:15036–15042
- Huang H, Wang Y, Ruditskiy A, Peng HC, Zhao X, Zhang L, Liu J, Ye Z, Xia Y (2014) ACS Nano 8:7041–7050
- 26. Xia Y, Xia X, Peng HC (2015) J Am Chem Soc 137:7947-7966
- 27. Zhang H, Jin M, Xia Y (2012) Chem Soc Rev 41:8035-8049
- 28. Bauer E, van der Merwe JH (1986) Phys Rev B 33:3657-3671
- Xia Y, Gilroy KD, Peng HC, Xia X (2017) Angew Chem Int Ed 56:60–95
- Sui S, Wang X, Zhou X, Su Y, Riffat S, Liu CJ (2017) J Mater Chem A 5:1808–1825
- 31. Xia Y, Halas NJ (2005) MRS Bull 30:338-348
- Choi S, Herron JA, Scaranto J, Huang H, Wang Y, Xia X, Lv T, Park J, Peng HC, Mavrikakis M, Xia Y (2015) ChemCatChem 7:2077–2084

Publisher's Note Springer Nature remains neutral with regard to jurisdictional claims in published maps and institutional affiliations.

